Phys Chem Minerals (2002) 29: 217–225
DOI 10.1007/s00269-001-0218-2

ORIGINAL PAPER

N. R. J. Poolton · K. B. Ozanyan · J. Wallinga
A. S. Murray · L. Bøtter-Jensen

Electrons in feldspar II: a consideration of the influence of conduction band-tail states on luminescence processes

Received: 11 May 2001 / Accepted: 6 September 2001

Abstract Most natural feldspars contain many charged impurities, and display a range of bond angles, distributed about the ideal. These effects can lead to complications in the structure of the conduction band, giving rise to a tail of energy states (below the high-mobility conduction band) through which electrons can travel, but with reduced mobility: transport through these states is expected to be thermally activated. The purpose of this article is twofold. Firstly, we consider what kind of lattice perturbations could give rise to both localized and extended conduction band-tail states. Secondly, we consider what influence the band tails have on the luminescence properties of feldspar, where electrons travel through the sample prior to recombination. The work highlights the dominant role that 0.04–0.05-eV phonons play in both the luminescence excitation and emission processes of these materials. It also has relevance in the dating of feldspar sediments at elevated temperatures.

Keywords Feldspar · Luminescence · Hopping transport · Mobility edge · Effective mass

N. R. J. Poolton (✉)
Synchrotron Radiation Department, Daresbury Laboratory, Daresbury, Warrington, Cheshire WA4 4AD, England
e-mail: n.r.j.poolton@dl.ac.uk

K. B. Ozanyan
Department of Electrical Engineering and Electronics, UMIST, PO Box 88, Manchester M60 1QD, England

J. Wallinga
The Netherlands Centre for Geo-Ecological Research (ICG), Faculty of Geographical Sciences, Utrecht University, PO Box 80115, 3508 TC, Utrecht, The Netherlands

J. Wallinga · A. S. Murray
Nordic Laboratory for Luminescence Dating, Department of Earth Sciences, Aarhus University, Risø National Laboratory, 4000 Roskilde, Denmark

L. Bøtter-Jensen
Nuclear Safety Research Department, Risø National Laboratory, 4000 Roskilde, Denmark

Introduction

Together with the preceding article (Electrons in feldspars I: on the wavefunction of electrons trapped at simple lattice defects), we are attempting to make an initial understanding of the properties and behaviour of electrons in feldspars. Whilst Part I considers the simple case of how an electron spreads out when trapped at a classic hydrogenic defect (referred to as the IRSL electron trap), this article seeks to consider how a free electron moves through the lattice. In both cases, the most readily accessible tools for testing the effects are via luminescence measurements, and the work has application to the luminescence dating of sediments.

The luminescence process that is of particular interest is one in which an electron, located at the IRSL trap, is stimulated optically to recombine with a hole located elsewhere in the lattice. We will assume that the hole is sufficiently far away for direct electron-hole recombination (arising through overlap of their wavefunctions) not to take place. As a consequence, the electron must pass through the conduction band in order to recombine; this electron, then, is to be our probe for examining the properties of the conduction band.

In the alkali feldspars, the depth of the IRSL electron trap's ground state is ~2 eV below the conduction band (see Part I). However, luminescence can be excited in the samples using photons of energy less than 2 eV in two ways:

1. In the infrared (IR) at ~1.5 eV a resonance is usually observed as the first excited state of the trap is accessed. The luminescence is thermally enhanced, with thermal activation energies in the range 0.02–0.15 eV typically being reported Rieser et al. 1997 (Bailiff and Barnett 1994; Bailiff and Poolton 1991; Poolton et al. 1995).
2. The 1.5-eV resonant peak is usually superimposed on a rising continuum, as the photo-excitation energy increases from 1 to 2 eV (e.g. Hütt et al. 1988; Poolton et al. 1995b; Jaek et al. 1997). The relative

intensity of this component (with respect to the resonance) and where the low-energy limit occurs, are sample-dependent.

Clearly, the thermal activation energies of 0.02–0.15 eV are too small to represent the energy bridge between the excited state and conduction band (~0.5 eV). However, the low-energy luminescence excitation continuum suggests that there may be a range of energy states available. We will be arguing in this article that these are band-tail states that lie below the high-mobility conduction band: the thermal dependence of the luminescence is explained by their presence, since they strongly affect the electron mobility.

Origin of the band tails in feldspars

The presence of just a single charged impurity or non-standard bond angle in an otherwise perfectly crystalline insulator or semiconductor will lead to an isolated deformation in the conduction band potential. Where there are many such imperfections, the potential fluctuations can form "band-tail" states where electron motion is still possible, but with reduced mobility: such tails extend above the valence, and below the conduction bands, into the forbidden gap (e.g. Redfield 1963a, b; Mott and Davis 1971).

For the wide band-gap silicates, we can gain an appreciation of the likely size of these effects from band-structure calculations. In the case of the various polymorphs of crystalline SiO_2, Li and Ching (1985) calculated that a variation of 10° in the Si–O–Si bond angle can lead to a change in the band gap of 0.65 eV: similarly, a bond-length variation of 0.1 Å was found to cause the gap to change by 3.5 eV. Later work by Xu and Ching (1991) confirmed the link between bond length and the energy gap.

Megaw (1974), in summarizing the structure of feldspars, discussed strain-induced variations in Si–O bond lengths, and O–Si–O bond angles within a typical feldspar lattice. In the latter case, a typical example of a bond-angle range from 103 to 116° (an average of about 109.5°) was given. As they are natural minerals, we also know that there are many impurity atoms typically present in feldspar (for sample analyses, see Deer et al. 1992) which will also contribute to localized conduction band fluctuations.

Figure 1 shows a schematic representation of the possible IRSL defect and conduction-band density of states in feldspar. The luminescence to be considered in the following sections arises from recombination at hole-trapping sites (not shown) after excitation from the ground state of the electron trap, either directly into the band-tail states or into the excited state (followed by transfer to the band tails).

Localization vs mobility in the band tails

In order to calculate the effects that lattice perturbations might have on electron behaviour in feldspar, we need a model to describe the situation. We will simplify this as much as possible, firstly by considering the solutions in 1-D (then transferring to 3-D), and secondly, by assuming that the perturbations are in the form of square potential wells. This basic model is not new. For example, in the seminal work of Anderson (1958), the energy of a crystalline material was modelled in 1-D by a series of square potential wells, with the potential fluctuations being tied in, by varying the well depths. In order to extract the information that is useful to us, however, it is possible to greatly simplify Anderson's model still further. We do this by providing a well-defined zero-point reference energy for the calculations (the conduction band edge E_c of the unperturbed lattice) and consider that the wells arise purely from the potential fluctuations appearing below E_c, as shown in Fig. 2a.

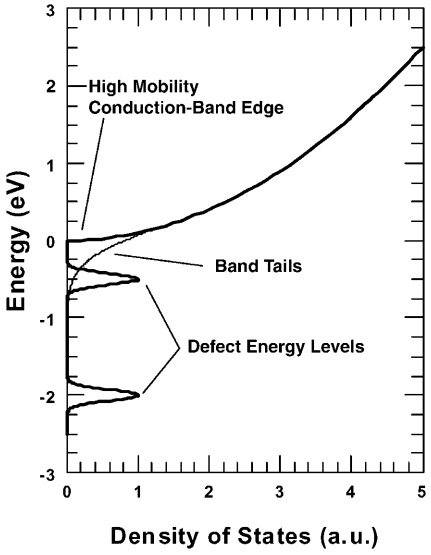

Fig. 1 Schematic diagram showing the relationship between the density of states of (1) the high-mobility conduction band, (2) the low-mobility band tails and (3) the IRSL electron trap's ground/excited state levels in alkali feldspar

In order to appreciate what affect such a potential might have on an electron, it is necessary to consider two points. Firstly, only certain energies are allowed for electrons within the wells: these energies depend on the well width, depth, effective electron mass and proximity of neighbouring wells. Secondly, the electron wave-function is not entirely confined within the well, but extends beyond the boundaries – as shown in Fig. 2b. This feature enables the electron to interact with, and transfer to, other wells elsewhere in the lattice.

The course of the following calculations is as follows: in the following section we first consider only isolated wells, and then weakly interacting wells of varying depth. This provides a basis for understanding thermally activated diffusion of electrons through the lattice. Later, we consider the more special case of strongly interacting wells, which lead to the appearance of extended electron states below E_c, and possible routes for more rapid electron diffusion through the lattice.

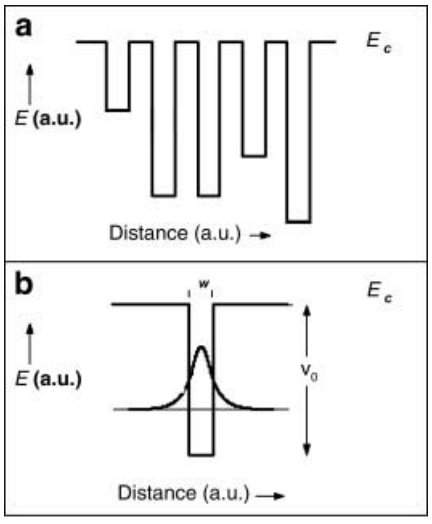

Fig. 2 **a** The conduction band energy fluctuations are approximated to square-well potentials below the high-mobility conduction band E_c. **b** Each well (of depth V_0 and width w) has at least one energy level associated with it: in isolated wells, this is well defined. Note that the wavefunction of an electron located in the well extends beyond the well boundaries, allowing the possibility of interacting with (and electron transfer to) other, neighbouring wells

Localized states: how they can arise

This section considers if it is realistic that quantum wells on the Å scale (e.g. as produced by bond length/angle variations) will lead to the occurrence of electron energy levels that could be accessed in IRSL. In particular, we are interested in those energy levels that lie in the range $E_c < E < (E_c - 0.5)$ eV, i.e. between the electron trap's excited state, and the conduction band (see the schematic of Fig. 1).

Finding the energy of the ground-state level in a 1-D square well of width w and finite depth V_0 (Fig. 2b) is a standard problem in quantum mechanics. It is most easily achieved from the Schrödinger equation that describes the situation (Bransden and Joachain 1989)

$$d^2\psi(x)/dx^2 + \alpha^2\psi(x) = 0 \ , \qquad (1)$$

where $\alpha = \left[8m_e^*\pi^2/h^2(V_0 - |E_c - E|)\right]^{0.5}$

by numerically solving

$$\gamma^2 - \xi^2 = (\xi \tan \xi)^2 \ , \qquad (2)$$

where $\xi = \alpha(w/2)$, and $\gamma = \left(2m_e^* V_0 w^2/h^2\right)$. m_e^* and h are the effective electron mass, and Planck's constant, respectively.

Figure 3a shows the solutions to Eq. (2), by continuously varying the well width from 0.5 to 20 Å, for three sample wells of depth $V_0 = 0.5$, 1.0 and 2.0 eV. This range of well widths covers all the important size ranges of interest, from the Si–O bond length (1.6 Å), to the *a*, *b*, *c* crystal cell parameters (8.1, 12.8, 7.2 Å respectively): these are figures for the Na-feldspar lattice, (e.g. Papike and Cameron 1976; Deer et al. 1992). The effective electron mass m_e^* has been directly determined from

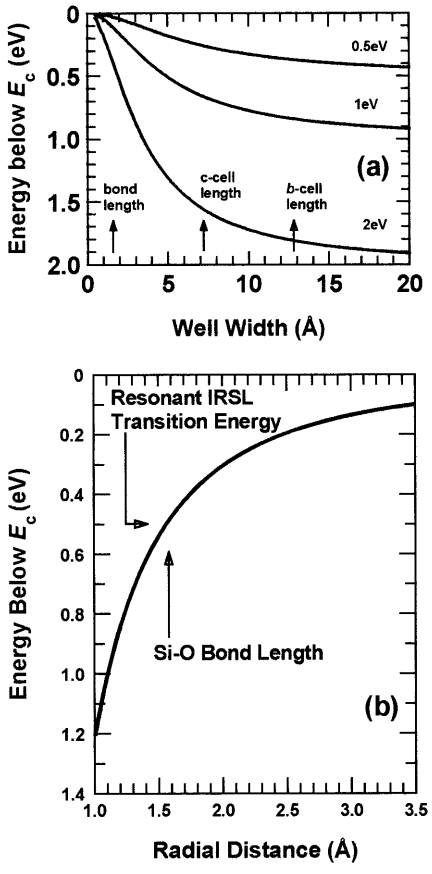

Fig. 3 **a** Plot of the ground-state energy positions for isolated wells of depth $V_0 = 0.5$, 1, 2 eV, as a function of the well width w. Comparison can be drawn between w and some important lattice parameters for Na-feldspar. **b** The wavefunction of an electron located in an isolated well extends beyond the well boundaries. The diagram shows (for alkali feldspar) at what radial distance beyond the well boundary the probability of finding the electron falls to $1/e$ of the value at the well boundary: this is plotted as a function of electron energy, below E_c

cyclotron resonance experiments to be 0.79 m_e (Poolton et al. 2001).

The significant feature of Fig. 3a is that ground-state energy levels close to $(E_c - 0.5)$ eV are present even in very narrow quantum wells of moderate depth (e.g. 1.6 Å, 2 eV; or 5 Å, 1 eV). A very realistic lattice perturbation might be anticipated on the scale of the spatial separation of two adjacent silicon atoms (~2.6 Å), for example. Here, a well depth of 1.5 eV would yield a ground-state electron level at $(E_c - 0.5)$ eV. Furthermore, no matter how narrow (or shallow) the well, there will always be at least one confined energy level appearing below E_c into which an electron can be excited.

Weakly interacting localized states: the route to electron mobility

In order to consider any mechanisms by which an electron in such a well can diffuse through the lattice

without accessing the high-mobility conduction band, it is necessary to appreciate that the electron is not totally localized within the well. Rather, the wavefunction extends beyond the well boundaries, falling off exponentially along the radial distance r, in the form:

$$\psi(r) = C\exp(-\beta r) \ , \tag{3}$$

C being a normalization constant. The variable β can be related to the electron energy, in the form (e.g. Bransden and Joachain 1989):

$$\beta = \left[8m_e^*\pi^2/h^2(E_c - E)\right]^{0.5} \ . \tag{4}$$

In Fig. 3b, we show how the tunnelling distance r is dependent on the energy of the electron, $E_c - E$. Here, r is taken as the distance from the well edge, where the probability $[\psi(r)]^2$ of finding an electron has fallen to $1/e$ of the value at the well edge. As m_e^* is unlikely to change in the Na–K feldspar range, Fig. 3 will be valid for all these materials. The figure shows that for smaller energies, the electron is very extensive, and can reach wells far removed.

In the case where the well is not isolated, but is adjacent to another well of equal depth, two regimes can be considered. When they are close enough, the calculated energy levels shown in Fig. 3a split and, if there are sufficient such wells, energy minibands occur, forming extended states. These are available for highly efficient sub-E_c electron transport, and we consider them in the next section in more detail. For the remainder of this section, we consider the case where the wavefunction overlap between wells is small. In this simpler case, the probability that hopping can occur from one well to another is also small, and the wavefunction overlap (and therefore hopping probability) can be approximated to $\exp(-2\beta R)$, R being the well-edge separations.

In the band tails, only a few adjacent wells are likely to be of the same energy (see Density of states). Rather, adjacent wells will tend to have larger (or smaller) energies. In this case, hopping is still possible if the electron receives (or yields) sufficient energy from the lattice, in the form of phonon absorption/emission, so as to match the electron energy level in the adjacent well. Note that in raising the energy by $\hbar\omega$, the overlap integral increases (or, from an alternative viewpoint, more distant wells can be accessed). We can say that, in general, the hopping probability P is thermally enhanced, and will be of the form:

$$P \propto \exp(-2\beta R)\exp(-\hbar\omega/kT) \ . \tag{5}$$

As pointed out by Mott (1973), this is directly related to the diffusion coefficient in the material, where there are many such wells, given as:

$$D = K\exp(-2\beta R)\exp(-\hbar\omega/kT) \ , \tag{6}$$

where K is a constant, whose value depends in part on the atomic coordination and the phonon frequency.

Since there is no preferred direction of motion, the electron can be considered to move in the form of a random walk. Thus, if after a certain time period it moves a lateral distance L ($\propto P$), the average volume V that it will have moved through in order to arrive at L is $(4/3)\pi L^3$. So, given a uniform distribution of recombination centres, the chances of the electron encountering a recombination centre on its walk are proportional to P^3. We use this result later when considering the luminescence intensity.

Extended states arising from multiple wells

Whilst the approach above is valid for weakly interacting wells where the interwell separation is large, more subtle effects occur if the wells become much closer. One such effect is to create highly efficient electron transfer channels in the material. In order to explore this, the simplest possible method is to consider the case of a 1-D series of quantum wells (QWs). We will give the wells realistic parameters, fixing V_0 (1.5 eV) and w (2.6 Å, approximately the Si–Si atomic separation), but vary the well separations continuously from 5 to 26 Å: this range covers the important *a, b, c* unit-cell parameters of the feldspars. All separating barriers are taken to be of equal width. The calculations directly follow that of Bastard et al. (1991) for multiquantum well structures.

Figure 4 summarizes the results of our calculations. At the largest barrier widths, the overlap between the wavefunctions in the separate QWs is low, and results in a single QW level at $(E_c - 0.48)$ eV. Note that this energy is exactly resonant with the excited state of the IRSL trap. As the barrier width decreases, the wavefunction overlap increases and the initially narrow level splits into a minizone. The latter is depicted in Fig. 4 by the band's upper and lower energy limits.

For a barrier width of 4.3 Å, the miniband width is 0.62 eV. For still narrower barriers, electrons can be activated from the miniband to E_c by absorption of a single phonon of energy $\hbar\omega \sim 0.05$ eV (this is a dominant phonon energy in feldspars: see below). However, for any barrier width less than 11.7 Å, the miniband becomes larger than this phonon energy. Consequently, in the range of barrier widths between 4.3 and 11.7 Å (outlined by dashed vertical lines in Fig. 4), phonon-assisted diffusion (PAD) can take place through the miniband. In this range, sequential hopping via the miniband states becomes sustainable because of suppressed ionisation probabilities (a multiphonon process will be required for activation into E_c) and favourable conditions for energy and momentum conservation in electron–phonon interactions (electrons may acquire momenta from phonons at the Brillouin-zone edges).

It is enlightening to compare the PAD range of barrier widths with the unit-cell constants for the typical case of Na-feldspar. Figure 4 shows that the lattice constants along all three crystallographic directions fall within the PAD range. Thus, it can be concluded that, within the suggested model, the PAD mechanism involves hopping ranges typical of that of the unit-cell lattice periods. The period at which the miniband

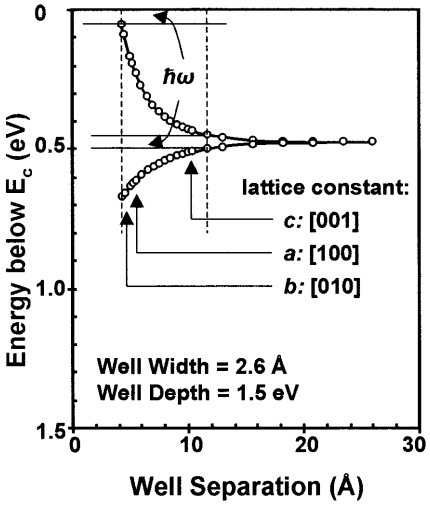

Fig. 4 Energy levels within a 1-D multiple quantum-well structure, calculated for a well width similar to the Si–Si atom separation and different well separations. The isolated $E_c - 0.48$ eV level splits into a miniband in the case of closer wells. Phonon-assisted diffusion by hopping to the adjacent cells along the principle crystallographic directions is possible in the region between 4.3 and 11.7 Å, indicated by the *two dashed vertical lines*. The *upper branch* of the miniband determines the ionisation energy from the well into the conduction band E_c, ranging from 0.05 to 0.45 eV

narrows to 0.05 eV is directly concordant with that of the *c* parameter, so that for a regular fluctuation in the unit cells, PAD could be envisaged to occur in a 1-D manner straight down the feldspar crankshaft axis.

Since the miniband energetically overlaps the calculated position of the excited state of the IRSL trap, direct electron transfer from the excited electron state into the miniband could be an alternative PAD-recombination channel. The transfer mechanism is likely to be very efficient, since the PAD range is also directly concordant with the radial extent of the excited electron wavefunction of the IRSL trap (see the work in Part I). With such an extensive wavefunction, direct recombination is possible with holes trapped elsewhere in the lattice, which would be both rapid and athermal. In contrast, PAD should exhibit longer lifetimes and be thermally activated, with phonon energies in the range 0.05 to 0.45 eV.

Density of states

We have already considered how or why a band-tail state might occur, having a particular energy E below the high-mobility conduction band edge, E_c. What we have not done yet is to assess how many such states might exist. This density of states is an important factor when considering the overall effect on processes such as electron conduction or luminescence. (If there is only one state in the whole lattice, obviously its impact is likely to be small).

Because the feldspars are essentially crystalline materials with some disorder (produced by imperfections, bond-angle and bond-length variations), it will not be possible to definitively describe the density of band-tail states for all cases. This will be very much sample-dependent: for example, it will be different for the same mineral with high or low structure. Here, we can examine possible or likely relationships between the energy and density of states.

Mott (1973) and Mott and Davis (1971) summarize several methods for calculating the density of states, $G(E)$. For example, where there is an infinite possibility of well-depth variation, then for large negative values of E, $G(E)$ could be of the form:

$$G(E) = |E| \exp\{-(4/3)|2E|^{1.5}\} \ . \tag{7}$$

However, as pointed out by Halperin and Lax (1966), experimentally, a range of $G(E)$ functions are observed, which can usually be approximated to the following relation

$$G(E) \propto \exp\{-|E|^n\} \ , \tag{8}$$

where n is in the range $0.5 < n < 2$.

The problem with these expressions is in placing the zero-point energy with respect to the high-mobility band edge E_c: the only case where this issue does not arise is where $n = 1$ in Eq. (8). For expedience, we will therefore consider the density of states to be of the form of Eq. (8), setting $n = 1$, but note that other possibilities are likely.

Consequences for luminescence

Luminescence intensity and thermal activation energies

Following the arguments above (Eqs. 5, 8), it is to be anticipated that the energy-resolved luminescence excitation spectra, involving excitation from the IRSL trap's ground state into the band-tail states, will follow the general temperature-dependent form:

$$I(E,T) \propto \exp\{-|E|\}[\exp[-2\beta(E)R] \exp(-\hbar\omega/kT)]^3 \ . \tag{9}$$

The form of this excitation spectrum is shown in Fig. 5a. [As an aside, note that in Eq. (9), the zero-point energy is the edge of the high-mobility conduction band edge, E_c. In exciting luminescence, however, electrons originate from the electron trap's ground state, so the photon excitation energies shown in Fig. 5 are in respect of this (i.e. $E_0 = E_c - 1.97$ eV for Na-feldspar, or $E_c - 1.99$ eV for K-feldspar: the difference arises due to the slightly different value of ε_r in the two materials)].

Comparing the proposed excitation spectrum of purely the band tails with experimental results is problematic, because of the overlap with the resonant Gaussian excitation spectrum, which often dominates the spectrum in the range 1.3–1.6 eV. (For the comparison shown in Fig. 5, an amalgam of previously reported data is used: see caption for sources). Where the two components have been deconvoluted in alkali

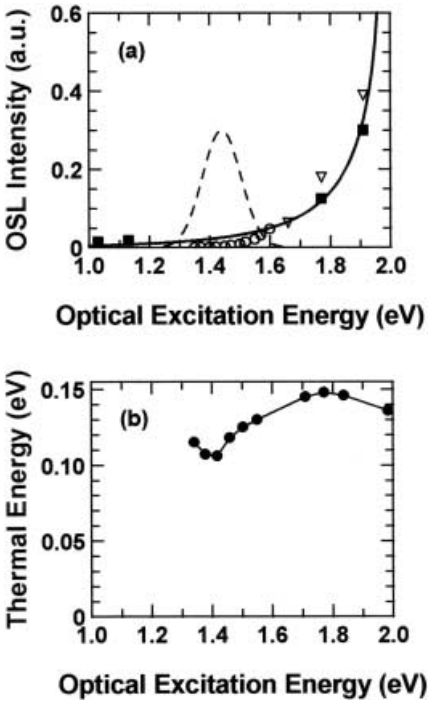

Fig. 5 **a** The *solid line* shows the calculated luminescence excitation spectrum of electrons from the IRSL trap's ground state in alkali feldspars, into band-tail states, at 300 K; the *dashed line* shows the location of the infrared resonance that is normally observed, overlapping the band-tail continuum. Comparison can be drawn with a variety of experimental results previously published for K-feldspar. ■ Bailiff and Poolton (1991), from the OSL bleaching of sanidine; ∇ Spooner (1994) from the OSL bleaching of microcline; ● Poolton et al. (1995b) deconvoluted from the OSL resonance-plus-continuum of orthoclase. **b** Excitation energy dependence of the thermal activation energy in orthoclase (after Poolton et al. 1995a). The tunnelling component of the luminescence in this sample is negligible, so the curve is thought to be principally representative of luminescence involving band-tail states

feldspars, the tail usually tends to disappear at an excitation energy of around 1.3–1.4 eV (i.e. 0.6–0.7 eV below E_c), although in some materials (such as highly disordered sanidine), there is evidence that the tails can extend to 1 eV below E_c.

Equation (9) also shows that the luminescence is thermally activated, and experimental measurements are shown in Fig. 5b for the case of orthoclase. We should point out that in the preceding article (Part I) we have shown that the thermal activation energy at the position of the IR resonance can fall to anomalously low values, due to tunnelling from the electron trap's excited state. Although the results shown in Fig. 5b do show a slight dip at 1.44 eV, there is little evidence of tunnelling in this sample and, furthermore, the resonance is weak compared with the non-resonant background: at 1.53 eV, for example, the contributions are equal. We believe, therefore, that Fig. 5b is a good general representation of the thermal dependence of the luminescence derived from the band tails.

To allow hopping, the activation energies can only be those of the lattice phonons available. For feldspars, these typically occur at 0.04–0.07, 0.09, 0.13, 0.14 eV (e.g. Salje 1993). The results of Fig. 5b show that the measured thermal activation energies [from Arrhenius plots Ln(I) vs $1/T$] lie between 0.11 and 0.15 eV over the stimulation range 1.3–2 eV. However, Eq. (9) shows that these values are three times the actual phonon energies involved. In other words, the phonons likely to play a part here are those with energies at 0.04–0.05 eV (in agreement with the discussion above). This is an interesting result, since these energies lie in a region of strong lattice vibration, and the same phonons have been shown to be dominantly responsible for the thermal quenching of a variety of luminescence processes in alkali feldspars (White et al. 1986; Poolton et al. 1995c; Barnett and Bailiff 1997).

Thermo-optical bleaching of OSL

The basis of luminescence dating of feldspar sediments is that the OSL centres are bleached by sunlight exposure during transport and accumulate charge during burial (through environmental radiation), and the amount of charge accumulated can be determined by OSL experiments in the laboratory (e.g. Aitken 1998). Although the basic concepts of this are simple, the presence of low-mobility conduction band-tail states in feldspars complicates matters. They restrict how far an excited electron of a particular energy can travel at any particular temperature (by the random-walk hopping process). Here, we start to explore the effects of this restricted mobility. In the following section, we show that it can have severe consequences for dating.

Figure 6a shows the thermal enhancement effects of OSL for a typical sedimentary K-feldspar under 1.49-eV excitation. Comparison of these curves shows that although the intensity increases with temperature, the form of the decay is largely unaffected (apart from a minor change in the early part of the decay). In other words, by and large,

$$I(t,T) \propto \exp(-W/kT)I(t) \ , \tag{10}$$

where W is the measured activation energy: similar results have been presented elsewhere (e.g. McKeever et al. 1997). Experimentally, the luminescence decay (under constant infrared (IR) stimulation) is generally found to be of the form (McKeever et al. 1997; Bailiff and Poolton 1991):

$$I(t) \propto (1+\gamma t)^{-n} \ , \tag{11}$$

where γ is a constant, and n is in the range $1 < n < 2$. Why this is so has never been adequately explained, and we do not seek to consider this aspect of the luminescence here.

If IR light is used to bleach the sediment, but the OSL is actually measured using higher excitation energies, the amount of bleaching is strongly dependent on the bleach temperature (Fig. 6b), with more luminescence being bleached at the higher temperatures. This contrasts with

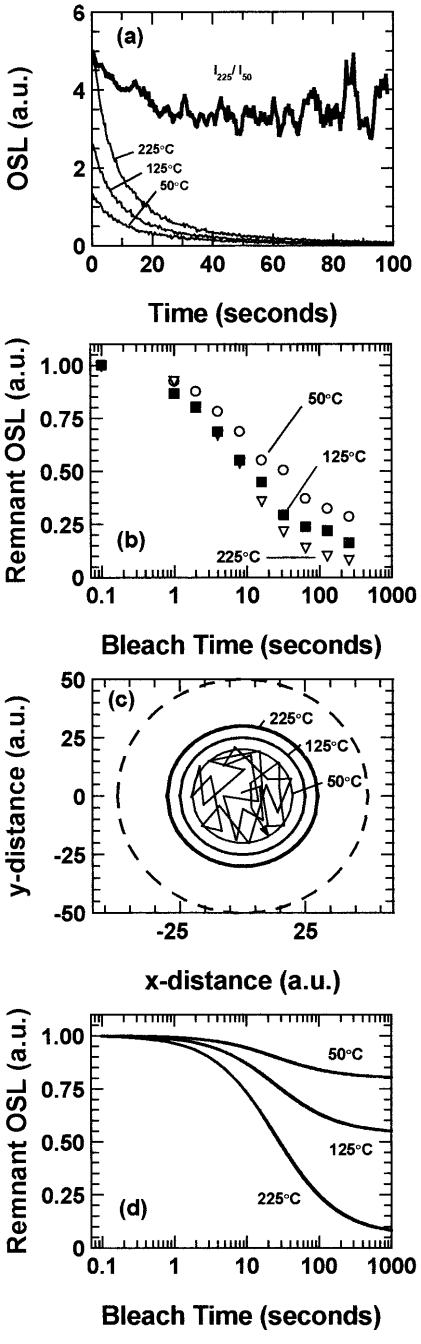

◀

Fig. 6 **a** The OSL decay curves of a sedimentary K-feldspar (sample from Leidschendam, The Netherlands level 1: see Wallinga et al. 2001) under 1.49 eV excitation energy, at various temperatures. The emission is thermally enhanced, but the rate of decay is largely unaffected (as indicated by the ratio of OSL measured at 50 and 225 °C), showing that more recombination centres are being accessed at higher temperature. **b** If the OSL in sedimentary K-feldspar is bleached at 1.49 eV prior to OSL measurement at higher stimulation energy (2.64 eV) the rate of bleaching is increased when the bleach temperature is increased, again suggesting that more recombination sites are accessed at elevated temperature. **c** In the band-tail random-walk model, a low-energy hopping electron at 50 °C passes through a certain volume of material. If the temperature is increased, the volume increases. Under higher energy stimulation approaching the high-mobility band edge (*dashed line*), the volume mapped out by the electron is larger, but limited by scattering processes. **d** Using the conceptual model of **c**, the broad features of the experimental bleach curves of **b** can be simulated, although the amount of bleaching at the lower temperatures is underestimated

the case where bleaching and OSL stimulation occur at the same wavelength: here, if the IR-OSL is measured at 50 °C but IR bleaching occurs at a sequence of higher temperatures, no variations in the degree of bleaching are observed.

The random-walk band-tail model largely accounts for the experimental observations outlined above. As schematically shown in Fig. 6c, at 50 °C an electron excited into the band-tail states undergoes a random walk, hopping from site to site with thermal assistance: as the temperature increases, the volume swept out by the electron increases (as Eq. (9), so more OSL is observed irrespective of time (Eq. 10). If OSL is performed at, say, 2 eV (the threshold for stimulation to E_c), the hopping length L does not tend to ∞ as suggested by Eqs. (3) and (4), but rather, it will be limited to a scattering length L_s. Thus, with excitation at or above E_c, the volume encountered by the electron is large, but limited (dashed curve in Fig. 6c). Consequently, one expects a larger volume of sample (accessible by high-energy stimulation) to be bleached by low-energy light when the sample is at elevated temperature. Taking values $W = 0.12$ eV $= 3\hbar\omega$, $\gamma = 0.04$, $n = 1$ in Eqs. (9), (10), (11) and with $L_s = 1.7L$ (at 50 °C, 1.5 eV excitation), the resultant bleaching behaviour shown in Fig. 6d is calculated. This clearly shows the same trend as the experimental results of Fig. 6b, and the broad features of the luminescence/bleaching behaviour are explainable. However, the model does underestimate the amount of bleaching happening at 50 °C compared with 225 °C, and there are probably a number of reasons why this is so. Firstly, we have assumed that the electrons are excited from the IRSL trap's ground state only into the band tails, and no account of the excited state is made. We have seen above, for example, that resonant electron transfer between the trap's excited state, and conduction minibands (which would produce more effective bleaching) is likely to be very efficient. Secondly, no account of the limiting factor $L \rightarrow L_s$ has been made in the model for IR-excited electrons at elevated temperatures. Much more experimental work is needed in determining electron lifetimes and the scattering lengths before a complete model can be provided.

Consequences for luminescence dating

These results have direct implications in the dating of sediments. We first consider the hypothetical situation where, at the time of deposition, the feldspars were exposed to the full sunlight spectrum during prolonged bleaching. To date, in this material using OSL, any stimulation wavelength in the range 400–900 nm (1.4–3.1 eV) could, in principle, be employable. However, if the sediments were bleached only with

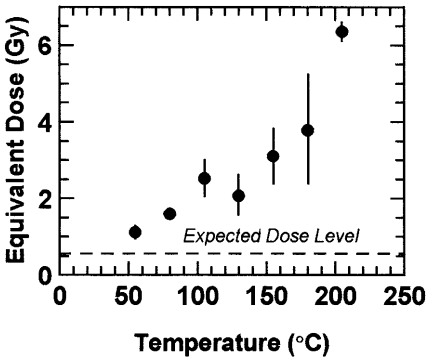

Fig. 7 Evaluated (equivalent) radiation dose in natural K-feldspar sediments (sample from Winssen, The Netherlands: see Wallinga et al. 2001), as a function of IR-OSL measurement temperature. (Each *point* is the average of three measurements, made using the SAR method: Wallinga et al. 2000). Through historical records, the sample is known to be 300 years old, allowing a calculation of the expected dose to be made (shown as the *dashed horizontal line*). Although elevated temperatures makes the sample luminescence brighter, it also makes the evaluated dose diverge from the expected value. This is probably due to enhanced thermal hopping processes of electrons in the band-tail states, allowing access to recombination sites not bleached during fluvial transport at ambient temperatures

low-energy light on deposition, then the results show that with high-energy OSL stimulation traps would be accessed that may not have been bleached during deposition – leading to an overestimate of the palaeodose. This situation is unlikely to occur in nature, since even in turbid, water-lain environments, the transmitted light spectrum tends to become narrowed, peaking around 580 nm, 2.1 eV (Berger 1990) – an energy large enough to ionise the electron traps.

Of much greater relevance is the suggestion of Duller and Wintle (1991) that for very weakly emitting samples accumulated doses might be assessed in materials using IRSL at elevated temperatures, to enhance the luminescence output. The results summarized in Fig. 6 suggest that this would be inappropriate, since charge would be accessed at the high measurement temperature that would not have been accessible during the bleaching process at much lower temperatures (because of the enhanced thermal-hopping processes). Again, an overestimation of the accumulated radiation dose would be evaluated. That this is so can be seen directly from Fig. 7, where, as an example, we have compared the evaluated dose for a K-feldspar extract of a fluvial deposit at a variety of measurement temperatures. Here, it is clearly seen that the evaluated dose rises sharply with measurement temperature; the most accurate dose measurement is the one made at a temperature closest to that at deposition (assumed to be around 10 °C). [This particular sediment, from the River Waal in The Netherlands, is 300 ± 20 years old; the age is known from historical documentation (Middelkoop 1997), and the expected dose in the sediment has been backcalculated from the measured dose rate (Wallinga et al. 2001)].

Conclusions

We have shown how minor fluctuations in alkali feldspar crystal lattices could lead to the presence of low-mobility band-tail states. The presence of these states can explain a number of features of optically stimulated luminescence in feldspar, including:

1. The presence and form of a long luminescence excitation continuum, extending in some cases to 1 eV below the high-mobility band edge.
2. The thermal enhancement behaviour of infrared stimulated luminescence, IRSL (which arises from thermally activated hopping among the band-tail states).
3. The low-energy optical bleaching behaviour of optically stimulated luminescence, OSL, excited at higher energy.
4. The incorrect dose evaluation in natural sediments, if OSL measurements are made at elevated temperature. This is due to thermally induced accessing of recombination centres not bleached at deposition.

The analysis shows that the thermal activation in alkali feldspars is controlled by lattice phonons in the energy range 0.04–0.05 eV, confirming the importance of these in controlling many aspects of both luminescence excitation and emission in feldspar materials.

Acknowledgements We wish to thank Dr. E. Bulur of the Technische Universitat Darmstadt for stimulating discussions on OSL phenomena in feldspars. J.W. thanks the Netherlands Organization for Scientific Research (NWO) for financial support.

References

Aitken MJ (1998) An introduction to optical dating. Oxford University Press, Oxford

Anderson PW (1958) Absence of diffusion in certain random lattices. Phys Rev 109: 1492–1505

Bailiff IK, Poolton NRJ (1991) Studies of charge transfer mechanisms in feldspars. Nucl Tracks Radiat Meas 18: 111–118

Bailiff IK, Barnett SM (1994) Characteristics of infrared-stimulated luminescence from a feldspar at low temperature. Radiat Meas 23: 541–545

Barnett SM, Bailiff IK (1997) The temperature dependence of luminescence in some feldspars (80–300 K). J Phys (D) Appl Phys 30: 683–689

Bastard G, Brum JA, Ferreira R (1991) Electronic states in semiconductor heterostructures. Solid State Phys 44: 229–415

Berger GW (1990) Effectiveness of natural zeroing of the thermoluminescence in sediments. J Geophys Res Solid Earth Planets 95(B8): 12375–12397

Bransden BH, Joachain CJ (1989) Introduction to quantum mechanics. Longman Scientific and Technical, Harlow, UK

Deer WA, Howie RA, Zussman J (1992) An introduction to the rock-forming minerals, 2nd edn. Longman Scientific and Technical, London

Duller GAT, Wintle AG (1991) On infrared stimulated luminescence at elevated temperatures. Nucl Tracks Radiat Meas 18: 379–384

Halperin BI, Lax M (1966) Impurity-band tails in the high density limit. I. Minimum counting methods Phys Rev 148: 722–740

Hütt G, Jaek I, Tchonka J (1988) Optical dating: K-feldspar optical response stimulation spectra. Quatern Sci Rev 7: 381–385

Jaek I, Hütt G, Vassiltchenko I (1997) Luminescence study of Eu- and Cu-doped natural alkali feldspars and quartz and some problems of palaeodosimetry. Radiat Meas 27: 473–477

Li YP, Ching WY (1985) Band structures of all polycrystalline forms of silicon dioxide. Phys Rev (B) 31: 2172–2179

McKeever SWS, Bøtter-Jensen L, Agersnap Larsen N, Duller GAT (1997) Temperature dependence of OSL decay curves: experimental and theoretical aspects. Radiat Meas 27: 161–170

Megaw H (1974) The architecture of the feldspars. In: The feldspars. MacKenzie WS, Zussman J (eds) Manchester University Press, Manchester, UK, pp 1–24

Middelkoop H (1997) Embanked floodplains in The Netherlands: geomorphological evolution over various time scales. Neth Geogr Stud 224: p 68

Mott NF (1973) In: Electronic and structural properties of amorphous semiconductors Ch. 1, ''Electrons in non-crystalline materials'' Le Comber PG, Mort L (eds) Academic Press, London, pp 1–54

Mott NF, Davis EA (1971) Electronic processes in non-crystalline materials. Clarendon Press, Oxford

Papike JJ, Cameron M (1976) Crystal chemistry of silicate minerals of geophysical interest. Rev Geophy Space Phys 14: 37–80

Poolton NRJ, Bøtter-Jensen L, Johnsen O (1995a) Thermo-optical properties of optically stimulated luminescence in feldspars. Radiat Meas 24: 531–534

Poolton NRJ, Bøtter-Jensen L, Johnsen O (1995b) Influence on donor electron energies of the chemical composition of K, Na and Ca aluminosilicates. J Phys Condensed Matter **7**: 4751–4762

Poolton NRJ, Bøtter-Jensen L, Duller GAT (1995c) Thermal quenching of luminescence processes in feldspars. Radiat Meas 24: 57–66

Poolton NRJ, Nicholls JE, Bøtter-Jensen L, Smith GM, Riedi PC (2001) Observation of free electron cyclotron resonance in $NaAlSi_3O_8$ feldspar: direct determination of the effective electron mass. Phys Stat Solidi (b) 225: 467–475

Redfield D (1963a) Electric fields of defects in solids. Phys Rev 130: 914–915

Redfield D (1963b) Effect of defect fields on the optical absorption edge. Phys Rev 130: 916–918

Rieser U, Hütt G, Krbetchek MR, Stoltz W (1997) Feldspar IRSL emission spectra at high and low temperatures. Radiat Meas 27: 273–278

Salje EKH (1993) Phase transitions and vibrational spectroscopy in feldspars. In: Feldspars and their reactions. Parsons I (ed) Kluwer Academic, Dordrecht, pp 103–106

Spooner NA (1994) The anomalous fading of infrared-stimulated luminescence from feldspars. Radiat Meas 23: 625–632

Wallinga J, Murray AS, Wintle AG (2000) The single-aliquot regenerative-dose (SAR) protocol applied to coarse-grain feldspar. Radiat Meas 32: 529–533

Wallinga J, Duller GAT, Murray AS, Törnqvist TE (2001) Testing optically stimulated luminescence dating of sand-sized quartz and feldspar from fluvial deposits. Earth Planet Sci Lett (in press)

White WB, Matsumura M, Linnehan DG, Furukawa T, Chandrasekhar BK (1986) Absorption and luminescence of Fe^{3+} in single-crystal orthoclase. Am Mineral 71: 1415–1419

Xu YN, Ching WY (1991) Electronic and optical properties of all polymorphic forms of silicon dioxide. Phys Rev (B) 44:11048–11059